Heterotetrameric Composition of Aquaporin-4 Water Channels†

John D. Neely,‡ Birgitte M. Christensen,§ Søren Nielsen,§ and Peter Agre*,‡

Departments of Biological Chemistry and Medicine, Johns Hopkins University School of Medicine, Baltimore, Maryland 21205, and Department of Cell Biology, Institute of Anatomy, University of Aarhus, 8000 Aarhus, Denmark

Received April 26, 1999; Revised Manuscript Received July 1, 1999

ABSTRACT: Aquaporin (AQP) water channel proteins are tetrameric assemblies of individually active ∼30 kDa subunits. AQP4 is the predominant water channel protein in brain, but immunoblotting of native tissues has previously yielded multiple poorly resolved bands. *AQP4* is known to encode two distinct mRNAs with different translation initiating methionines, M1 or M23. Using SDS−PAGE urea gels and immunoblotting with anti-peptide antibodies, four polypeptides were identified in brain and multiple other rat tissues with the following levels of expression: 32 kDa > 34 kDa > 36 kDa > 38 kDa. The 34 and 38 kDa polypeptides react with an antibody specific for the N-terminus of the M1 isoform, and 32 and 36 kDa correspond to the shorter M23 isoform. Immunogold electron microscopic studies with rat cerebellum cryosections demonstrated that the 34 kDa polypeptide colocalizes in perivascular astrocyte endfeet where the 32 kDa polypeptide is abundantly expressed. Velocity sedimentation, cross-linking, and immunoprecipitation analyses of detergent-solubilized rat brain revealed that the 32 and 34 kDa polypeptides reside within heterotetramers. Immunoprecipitation of AQP4 expressed in *Xenopus laevis* oocytes demonstrated that heterotetramer formation reflects the relative expression levels of the 32 and 34 kDa polypeptides; however, tetramers containing different compositions of the two polypeptides exhibit similar water permeabilities. These studies demonstrate that AQP4 heterotetramers are formed from two overlapping polypeptides and indicate that the 22-amino acid sequence at the N-terminus of the 34 kDa polypeptide does not influence water permeability but may contribute to membrane trafficking or assembly of arrays.

Aquaporin water channel proteins have been identified in multiple mammalian tissues as well as in invertebrates, plants, and microorganisms (*1*). Known mammalian aquaporins are selectively permeated by water (orthodox aquaporins) or water and glycerol (aquaglyceroporins). While little is known about the regulation of water channel expression and function, it is becoming clear that the amino acid sequences of different aquaporins contain motifs needed to function in specific tissues or subcellular compartments. The three-dimensional structure of AQP1[1] has been determined at 6 Å resolution (*2*−*4*), and aquaporin sequences are being investigated so the molecular determinants of water permeability, channel selectivity, and regulation can be delineated (*5*, *6*). AQP1 exists as a homotetramer in red blood cells (*7*−*9*), and mutations which disrupt subunit oligomerization prevent the expression of water transport activity (*10*). Also, AQP1 subunits with certain C-terminal deletions co-oligomerize with other mutant forms of AQP1 and restore function (*11*), whereas AQP2 subunits with certain C-terminal substitutions co-oligomerize with wild-type subunits and impair cellular trafficking (*12*).

The cDNA encoding AQP4 was cloned from rat lung (*13*) and brain (*14*). AQP4 is also expressed in other tissues, including renal collecting duct, secretory glands, fast-twitch fibers in skeletal muscle, and stomach (*15*−*20*). In the central nervous system, AQP4 is expressed in astrocytes, ependymal cells, and retinal Müller cells (*16*, *21*, *22*), where the protein may facilitate water fluxes accompanying potassium siphoning and may regulate water permeability at the blood−brain barrier. *AQP4* is the only aquaporin thought to encode naturally occurring isoforms. Two rat AQP4 mRNAs which differ at their 5′ ends were identified, and cRNAs for both transcripts produced water transport activity when expressed in *Xenopus* oocytes (*14*). In vitro translation of these cRNAs in microsomes resulted in ∼30 kDa polypeptides which differed by ∼2 kDa, in agreement with the sizes of 32 and 34 kDa deduced from the cDNA sequences. These two polypeptides were predicted to arise in vivo from alternative transcripts and different translation initiating methionines, M1 or M23 (Figure 1). Analysis of *AQP4* genomic DNA and cDNA sequences from humans and mice have confirmed the existence of transcripts corresponding to M1 and M23 isoforms (*23*−*26*).

Several groups of investigators using antibodies specific for the C-terminus of AQP4 have shown the presence of a

† Supported by research grants from the National Institutes of Health and the Cystic Fibrosis Foundation (P.A.); also supported by the Novo Nordic Foundation, the Karen Elise Jensen Foundation, the Danish Medical Research Council, and the Biomembrane Research Center at the University of Aarhus (S.N.).

* To whom correspondence should be addressed: Department of Biological Chemistry, Johns Hopkins University School of Medicine, 725 N. Wolfe St., Baltimore, MD 21205. Telephone: (410) 955-7049. Fax: (410) 955-3149. E-mail: pagre@jhmi.edu.

‡ Johns Hopkins University School of Medicine.

§ University of Aarhus.

[1] Abbreviations: AQP, aquaporin; P_f, coefficient of osmotic water permeability (centimeters per second); PMSF, phenylmethanesulfonyl fluoride; SDS−PAGE, sodium dodecyl sulfate−polyacrylamide gel electrophoresis.

10.1021/bi990941s CCC: $18.00
Published on Web 08/03/1999

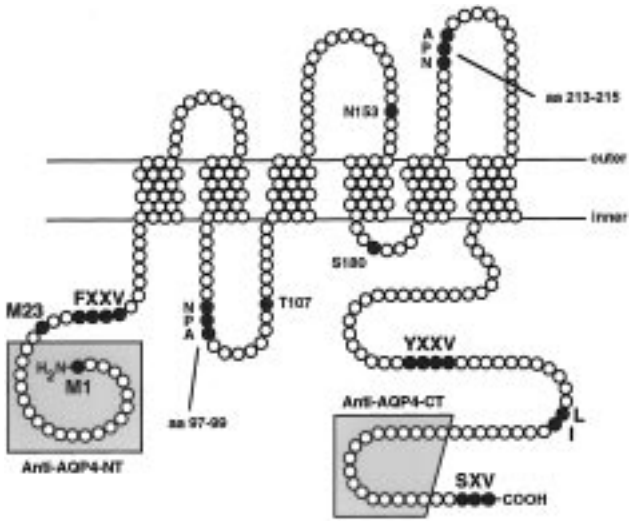

FIGURE 1: Schematic illustration of AQP4 structural motifs. The membrane topology of AQP4 was predicted by hydropathy analysis of the amino acid sequence deduced from cDNA (*14*). Initiating methionines for the M1 and M23 isoforms are denoted. Structural motifs with important known or potential roles in AQP4 function are also denoted: FXXV, YXXV, and LI, internalization motif consensus sequences; C-terminal SXV, PDZ-binding motif; T107 and S180, protein kinase C phosphorylation consensus sites; N153, glycosylation consensus site; and NPA97−99 and NPA213−215, aquaporin hemichannel signatures. Shaded boxes represent the peptide sequences recognized by the N-terminal (anti-AQP4-NT) or C-terminal antibody (anti-AQP4-CT).

major band at ∼30 kDa on immunoblots from all tissues where AQP4 is expressed. Multiple other bands ranging from 25 to >60 kDa have been observed but are poorly resolved. Bands of ∼30 and ∼32 kDa were described in whole rat brain (*16*), and rat cerebellum exhibited multiple bands at 31, 34, 59, and 64 kDa (*24*). A recent study of skeletal muscle (*19*) demonstrated the expression of ∼30 and 32 kDa AQP4 polypeptides but showed that the 25 kDa band represents an unrelated protein.

It remains unclear how many different AQP4 polypeptides are actually expressed in native tissues and whether they interact during assembly of subunits into tetramers. Since different AQP4 isoforms may have different functions or regulatory mechanisms, coherent recognition of their expression and oligomerization patterns is essential for understanding the biological roles of the protein. Here we employed SDS−PAGE with urea in the gels and performed immunoblotting with anti-peptide antibodies corresponding to the N- and C-termini of AQP4. Our studies demonstrate the presence of two major AQP4 isoforms which differ at their N-termini and coexist in heterotetramers. These studies suggest that some features unique to AQP4, such as the restricted protein distribution in perivascular astrocytes or incorporation into orthogonal arrays, may be determined by the asymmetry of this heterotetrameric protein.

MATERIALS AND METHODS

Tissue Membrane Preparations. Adult Sprague-Dawley rats (>300 g) were sacrificed, and isolated tissues were thoroughly homogenized at 4 °C with a 10 mL Potter-Elvehjem tissue grinder in at least 10 volumes of tissue homogenization buffer [7.5 mM sodium phosphate (pH 7.0), 0.25 M sucrose, 5 mM EDTA, and 5 mM EGTA] containing 0.7 μM aprotinin, 10 μM leupeptin, 7 μM pepstatin A, and 2 mM phenylmethanesulfonyl fluoride (PMSF). Homogenates were centrifuged for 10 min at 1000*g* and 4 °C, and the resulting supernatants were centrifuged for 30 min at 200000*g* and 4 °C, yielding the membrane fractions in the pellets.

Antibody Preparation. Anti-AQP4 antibodies were affinity-purified from rabbit immune serum. The C-terminal antibody (anti-AQP4-CT, LL182), described previously (*17*), was generated against a peptide consisting of rat AQP4 (GenBank accession number U14007) residues 302−318 with an added N-terminal cysteine (NH_2-CIDIDRGDEKK-GKDSSGE-COOH). The immunizing peptide for the N-terminal antibody (anti-AQP4-NT, LL431) was identical to rat AQP4 residues 1−21 except that the initial methionine was replaced by cysteine (NH_2-CSDGAAARRWGKCGP-PCSRES-COOH).

Electrophoresis and Immunoblotting. Tissue membrane fractions were solubilized at 37 °C for 30 min in 5.0% SDS, 20 mM Tris (pH 8.0), and 5 mM EDTA. Protein concentrations were determined using bicinchoninic acid (BCA Protein Assay Reagent, Pierce Chemical Co., Rockford, IL), and the samples were adjusted to concentrations of 1−2 μg of protein/μL in SDS−PAGE sample buffer [3.0% SDS, 10 mM Tris (pH 6.8), 6.0% glycerol, 0.01% bromophenol blue, and 0.1 M dithiothreitol]. Samples were analyzed by SDS−PAGE in slab gels with 4.0% acrylamide/2.0 M urea stacking sections and 12% acrylamide/4.0 M urea resolving sections (*27*). Inclusion of urea in the gels was required to obtain optimal resolution of AQP4. After electrophoresis, proteins were transferred to a poly(vinylidene difluoride) membrane, and blots were incubated for ∼12 h at 4 °C with affinity-purified rabbit antibodies (0.3 μg/mL anti-AQP4-CT or 1.4 μg/mL anti-AQP4-NT). Immunoreactive proteins were visualized by chemiluminescent detection using peroxidase-conjugated goat anti-rabbit IgG and ECL Plus (Amersham Pharmacia Biotech, Inc., Piscataway, NJ). The equivalency of protein sample applications was assessed by Coomassie Blue staining of gels.

Immunogold Electron Microscopy. Brains from adult Sprague-Dawley rats were perfusion-fixed with 0.1% glutaraldehyde/2% paraformaldehyde in 0.1 M sodium cacodylate buffer and postfixed for 30 min. Tissue blocks prepared from cerebellum were infiltrated for 30 min with 2.3 M sucrose containing 2% paraformaldehyde, mounted on holders, and rapidly frozen in liquid nitrogen (*18*). Immunolabeling was performed on ultrathin cryosections incubated overnight at 4 °C with anti-AQP4-NT diluted in PBS with 0.1% BSA or 0.1% nonfat milk. Labeling was visualized with goat anti-rabbit IgG conjugated to 10 nm colloidal gold particles (GAR.EM10, BioCell Research Laboratories, Cardiff, U.K.) diluted 1:50 in PBS with 0.1% BSA. Sections were stained with uranyl acetate and lead citrate before examination in a Philips CM100 or Philips 208 electron microscope.

Solubilization of Rat Brain AQP4. Digitonin, BRIJ 35, *n*-dodecyl β-D-maltoside, *n*-octyl β-D-glucopyranoside, CHAPS, sodium cholate, sodium deoxycholate, sodium lauroylsarcosine, and sodium *n*-dodecyl sulfate (SDS) were analyzed in 4% solutions for their ability to solubilize AQP4 in rat cerebellum membranes. After the membranes were incubated with detergent for 1 h at 37 °C, the solubility was assessed by partition of AQP4 into a 200000*g* supernatant. On the basis of this criterion, AQP4 from rat cerebellum

was insoluble in BRIJ 35 and cholate, soluble in deoxycholate as well as lauroylsarcosine and SDS, and partially soluble in the other detergents. Increasing the incubation temperature to 60 °C caused formation of SDS-insoluble aggregates. Deoxycholate was used for most experiments.

Differential Velocity Centrifugation. Half of the tissue membrane fraction from an adult rat cerebellum (organ mass of 260 mg) was solubilized in 2−3 mL of buffer containing 20 mM HEPES (pH 8.0), 4% sodium deoxycholate, 5 mM EDTA, 5 mM EGTA, 0.7 μM aprotinin, 10 μM leupeptin, 7 μM pepstatin A, and 2 mM PMSF by incubation at room temperature for 30 min and then at 37 °C for 1 h. The solubilized material was centrifuged for 30 min at 200000*g* at 4 °C. Supernatant aliquots of 100 μL were loaded onto 4.2 mL 5 to 20% linear sucrose gradients containing 20 mM HEPES (pH 8.0), 0.2% sodium deoxycholate, 5 mM EDTA, and 5 mM EGTA in 13 mm × 51 mm polypropylene copolymer thin-wall Ultra Tubes (Nalge Nunc International, Naperville, IL). Size standards [cytochrome *c*, carbonic anhydrase, bovine serum albumin (BSA), β-amylase, and catalase] were analyzed in a separate tube. Gradients were centrifuged for 16 h at 139000*g* in a Beckman SW50.1 rotor at 8 °C, and 200 μL fractions were collected from the top of each gradient.

Chemical Cross-Linking. To 400 μL of pooled fractions (9−12) was added 200 μL of buffer containing 0.45 mM DSP [dithiobis(succinimidyl propionate)], 20 mM HEPES (pH 8.0), and 0.2% sodium deoxycholate, for a final concentration of 150 μM DSP in 600 μL. After the sample was incubated at 4 °C for 30 min, cross-linking was terminated by the addition of ethanolamine [32 μL of 1 M ethanolamine (pH 8)] to a final concentration of 50 mM. On the basis of a Dreiding model of the structure of DSP, the range of possible cross-linking distances (from amide N to amide N) was estimated to be 4.5−11.6 Å.

Immunoprecipitation of Tetrameric AQP4 from Brain. To 400 μL of pooled fractions was added either 1 μg of anti-AQP4-CT, 3 μg of anti-AQP4-NT, or 3 μg of rabbit nonspecific IgG. Following incubation of the samples at 4 °C for 12 h, antigen−antibody complexes were precipitated by incubation at 4 °C for 1 h with 50 μL of BSA-blocked protein A−Sepharose CL-4B. Subsequently, the protein A−Sepharose was pelleted, and the supernatants were saved. The protein A−Sepharose was washed four times at 4 °C with buffer containing 20 mM HEPES (pH 8.0), 150 mM NaCl, 0.2% Triton X-100, 5 mM EDTA, and 5 mM EGTA. Antigen−antibody complexes were dissociated from the protein A−Sepharose by incubation at 37 °C for 30 min in 50 μL of SDS−PAGE sample buffer. Immunoprecipitates were analyzed by electrophoresis and immunoblotting. Due to instability of detergent-solubilized AQP4, we were unable to perform sequential immunoprecipitations or analyze supernatants after prolonged antibody incubations due to the appearance of high-molecular mass aggregates.

Immunoprecipitation of AQP4 from Skeletal Muscle. Extensor digitorum longus muscles from four sacrificed rats were dissected and combined (total tissue mass of 900 mg). Tissue was homogenized using a Brinkmann Polytron instrument with a PTA-10TS generator in 15 mL of ice-cold tissue homogenization buffer containing Boehringer Mannheim Complete Protease Inhibitor Cocktail tablets (Boehringer Mannheim Corp., Indianapolis, IN). Homogenates were centrifuged for 10 min at 1000*g* at 4 °C, and the supernatants were centrifuged at 2000*g*. To the 2000*g* supernatant were added 10 mM HEPES (pH 7.5), 150 mM NaCl, 0.1% Triton X-100, and 1.0% BSA. Following incubation at 4 °C for 1 h, the samples were centrifuged for 15 min at 20000*g* and 4 °C. To 1.0 mL of the 20000*g* supernatant was added 3 μg of anti-AQP4-CT or rabbit nonspecific IgG, and the resulting samples were analyzed essentially as described above for immunoprecipitation from brain.

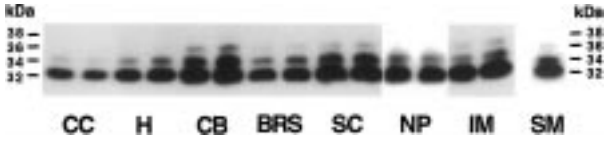

FIGURE 2: Tissue distributions of AQP4 in rats. Immunoblots of membrane proteins from brain, nasopharynx, and kidney (20 μg of protein/lane) or of protein immunoprecipitated from skeletal muscle with C-terminal antibody. Samples were separated by SDS−PAGE and analyzed on immunoblots reacted with C-terminal antibody. CC, cerebral cortex; H, hippocampus; CB, cerebellum; BRS, brainstem; SC, spinal cord; NP, nasopharynx; IM, renal inner medulla; SM, skeletal muscle extensor digitorum longus.

Heterologous Expression and Functional Studies. Rat *AQP4* cDNA (GenBank accession number U14007) was used to subclone the coding regions for M1 (base pairs −9 to 1310) and M23 (base pairs 7−1310) into the *Xenopus* oocyte expression construct pXβG (*14*). The resulting plasmids were linearized with *Xba*I, and capped RNA transcripts were synthesized as described previously (*28*, *29*). Defolliculated stage V−VI oocytes from *Xenopus laevis* were injected with 5 ng of cRNA or an equal volume (50 nL) of water, and swelling assays were performed 3 days later to determine osmotic water permeabilities (*28*, *29*).

Immunoprecipitation from AQP4-Expressing Xenopus Oocytes. AQP4-expressing oocytes were lysed by agitation in 100 μL per oocyte of ice-cold buffer containing 7.5 mM sodium phosphate (pH 7.0), 1 mM EDTA, 0.7 μM aprotinin, 10 μM leupeptin, 7 μM pepstatin A, and 2 mM PMSF. Lysates were centrifuged at 735*g* for 5 min at 4 °C, and the resulting supernatants were centrifuged at 16000*g* for 30 min at 4 °C, yielding the oocyte membranes in the pellets. Membranes were solubilized by incubation at 37 °C for 2 h in 20 μL per 10-oocyte membrane pellet of 20 mM Tris (pH 8.0), 10% glycerol, 2.0% sodium deoxycholate, 5 mM EDTA, 0.7 μM aprotinin, 10 μM leupeptin, 7 μM pepstatin A, and 2 mM PMSF. Solubilized samples were then centrifuged at 16000*g* for 30 min at 4 °C. Affinity-purified antibodies were added to 20 μL supernatant aliquots, and the final volumes were adjusted to 40 μL with water. The resulting samples were analyzed as described above.

RESULTS

Distribution of AQP4 Polypeptides in Different Tissues. To assess the relative abundance of different AQP4 polypeptides, several rat tissues were analyzed by SDS−PAGE and immunoblotting with an antibody that recognizes the AQP4 C-terminus (Figures 1 and 2). These tissues included cerebral cortex, hippocampus, cerebellum, brainstem, spinal cord, nasopharynx, renal inner medulla, and skeletal muscle. Since AQP4 in crude membrane preparations from skeletal muscle extensor digitorum longus could not be easily detected by

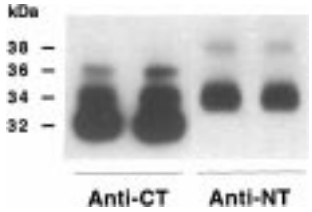

FIGURE 3: Recognition of 34 and 38 kDa polypeptides by the N-terminal antibody. The rat cerebellum membrane fraction (10 μg of protein/lane) was separated by SDS−PAGE and analyzed on immunoblots reacted with the C-terminal antibody (anti-AQP4-CT) or the N-terminal antibody (anti-AQP4-NT).

direct immunoblotting, the protein was first immunoprecipitated from skeletal muscle using the C-terminal antibody to increase detection sensitivity.

Previous studies with AQP4 have reported the presence of multiple poorly resolved bands in immunoblots. The resolution of AQP4 polypeptides was improved by solubilizing gel samples at 37 °C to minimize the formation of SDS-insoluble aggregates and by including urea in the SDS−PAGE gels. Immunoblots prepared with these methods exhibited four distinct bands: 32, 34, 36, and 38 kDa (Figure 2). AQP4 is most abundant in cerebellum, spinal cord, and renal inner medulla. Although the abundances of AQP4 in these tissues are not identical, the intensity of the four polypeptides relative to each other is consistent. In all of the tissues that were analyzed, the 32 kDa band is most abundant and the 34 kDa band is next most abundant. The 36 kDa band is weak, and prolonged photographic exposure is required to reveal the 38 kDa band (barely visible in Figure 2). Densitometric analyses of multiple blots showed that these polypeptides are present in approximately the following proportions: 1.0 (32 kDa), 0.14 (34 kDa), 0.05 (36 kDa), and 0.01 (38 kDa). A faint blur at ~70 kDa which sometimes appeared may represent SDS-insoluble AQP4 oligomers, but no other bands were visible.

Delineation of Different AQP4 Isoforms. A rabbit polyclonal antibody was raised to a peptide corresponding to the first 21 N-terminal amino acids of the deduced sequence of the rat AQP4 M1 isoform (Figure 1). The N-terminal antibody reacts only with the 34 and 38 kDa bands on immunoblots of rat cerebellum membranes (Figure 3). The 32 and 34 kDa bands correspond to the sizes deduced from the M23 and M1 cDNAs, and the specific recognition of the 34 kDa band by an antibody to the N-terminus of the M1 isoform indicates that the 32 and 34 kDa bands represent the M23 and M1 polypeptides. The minor bands at 36 and 38 kDa in immunoblots of native tissues seemingly represent post-translationally modified M23 and M1 polypeptides, although the specific modification is yet uncertain. SDS/Triton X-100-solubilized cerebellum membranes were treated with peptide:*N*-glycosidase F (PNGase F), but the coincidence of the size of the enzyme with that of the putative subtrates precluded interpretation (not shown). Cerebellum membranes were also treated with alkaline phosphatase, but the treatment failed to alter the mobilities of the four bands (not shown). The minor 36 and 38 kDa bands were not found in immunoblots of membranes prepared from oocytes injected with M1 or M23 cRNAs, even when the oocytes were treated with phorbol 12,13-dibutyrate (PDBu) at concentrations which achieved 50% downregulation of the osmotic water permeability (not shown).

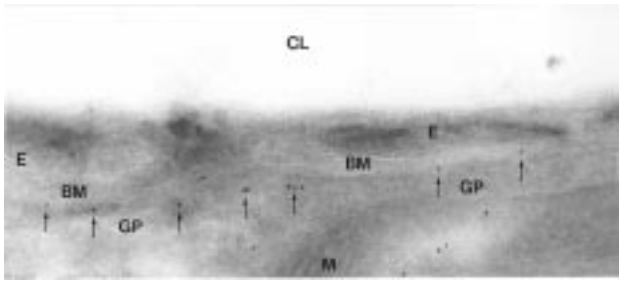

FIGURE 4: Subcellular distribution of the AQP4 34 kDa polypeptide in rat brain. Postembedding immunogold labeling with N-terminal antibody was performed on ultrathin cryosections of rat cerebellum. Immunogold labeling (arrows) is associated with perivascular astrocyte processes (glial processes, GP). No labeling appears in glial processes facing neuropil or in the capillary endothelium (E). CL, capillary lumen; M, mitochondria; BM, basement membrane. The magnification was 85500×.

Subcellular Localization of the AQP4 34 kDa Polypeptide in Rat Brain. Identification of separate molecular populations implies functional heterogeneity. Expression of two AQP4 isoforms in the same tissues raises the question of whether the 32 and 34 kDa polypeptides are expressed in different cell types or whether they are targeted to different subcellular sites within an individual cell. To investigate the cellular and subcellular localization of the 34 kDa polypeptide, the N-terminal antibody was used in immunogold electron microscopy of rat cerebellum. Pronounced labeling with the N-terminal antibody demonstrated that the 34 kDa polypeptide is present in the endfeet of astrocytes surrounding capillaries (Figure 4). Within these cells, labeling is found almost exclusively in membrane regions adjacent to the basement membrane. This distribution is identical to that shown previously using the C-terminal antibody (*21*), but the labeling with the N-terminal antibody is considerably less intense and may reflect a lower antibody affinity as well as a lower level of protein expression.

Differential Velocity Sedimentation of Rat Brain AQP4. The composition of channel subunits can potentially influence regulation or permeation. Thus, a biochemical approach based on solubilizing AQP4 in a tetrameric state was established to directly determine whether AQP4 forms separate species of homotetramers or whether AQP4 forms heterotetramers with mixed subunit composition. AQP4 from rat cerebellum solubilized with deoxycholate was subjected to differential velocity centrifugation in 5 to 20% linear sucrose gradients. Immunoblot analyses of the gradient fractions and comparisons to size standards revealed a single AQP4 peak at ~6.8 S (Figure 5A). This protein size is somewhat larger than the ~5.7 S size reported for Triton X-100-solubilized human AQP1 (*7*). Analyses of rat brain AQP4 performed in other detergents yielded size estimates as small as 5.2 S (not shown). Thus, the apparent size differences may reflect differences in detergent characteristics rather than actual differences in the size of the AQP4 protein. Importantly, these studies confirm that AQP4 retains the tetrameric oligomerization characteristic of other aquaporins.

Chemical Cross-Linking of Rat Brain AQP4. Chemical cross-linking of deoxycholate-solubilized AQP4 combined with SDS−PAGE analysis was used to further resolve the oligomeric structure of rat brain AQP4. Peak fractions from the sucrose gradients were combined and treated with DSP, a homobifunctional cross-linker with a mercaptan-cleavable

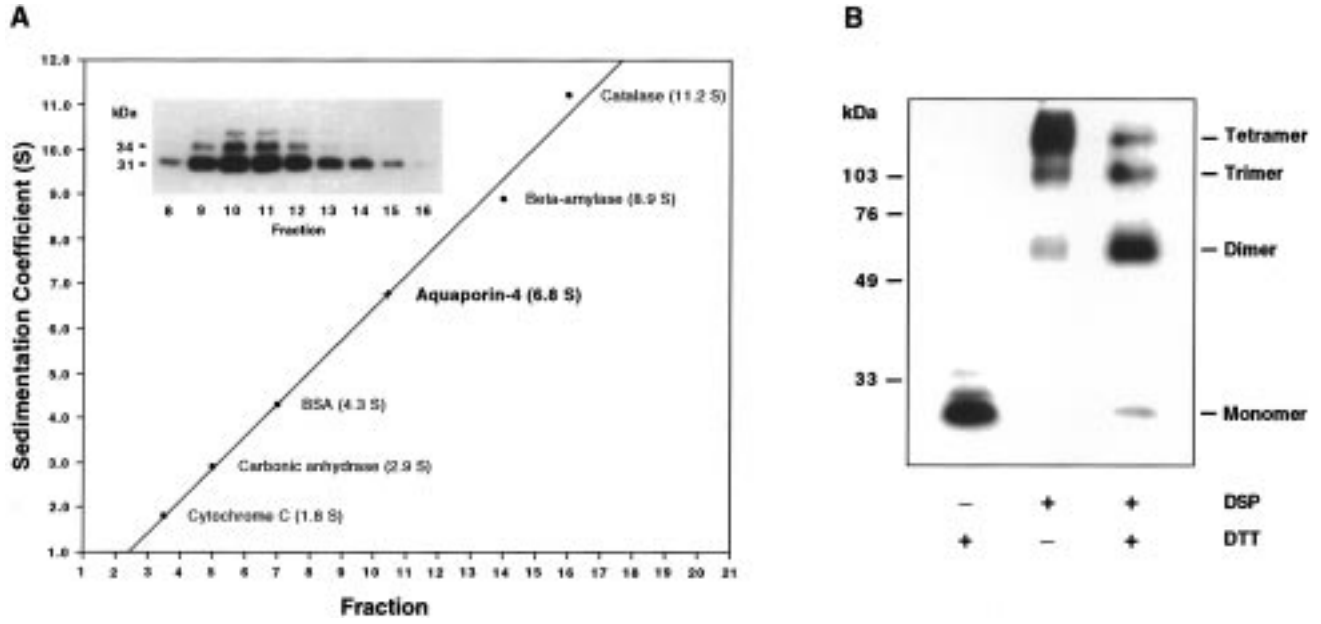

FIGURE 5: Sucrose gradient sedimentation of solubilized rat brain AQP4. (A) AQP4 from rat cerebellum was solubilized in deoxycholate and layered over 5 to 20% sucrose gradients. After 16 h at 139000*g*, gradient fractions were analyzed by SDS−PAGE and Coomassie Blue staining (for the molecular mass standards) or immunoblotting with the C-terminal antibody. The AQP4 particle size was determined on the basis of a linear regression analysis of the standards. (B) Peak gradient fractions (9−12) were combined and treated with 150 mM DSP for 30 min (4 °C), with or without subsequent addition of 0.1 M dithiothreitol (DTT). Samples were then separated by SDS−PAGE (10% acrylamide), and immunoblots were reacted with the C-terminal antibody.

intramolecular bond. Analysis of the peak fractions in the absence of DSP yielded bands at ~30 kDa as expected for monomeric, SDS-dissociated AQP4 (Figure 5B). In contrast, when the samples were incubated with DSP before SDS−PAGE and immunoblotting, a predominant band of >100 kDa was observed. Other less prominent bands were also noted at ~100 and ~60 kDa, but no other bands were present in the stacking gel or at the interface between the stacking and resolving gels. The estimated sizes of these bands roughly match the expected sizes of AQP4 if cross-linking occurred with variable efficiencies, yielding a mixture of dimers, trimers, and tetramers. Incubation of DSP-cross-linked AQP4 with dithiothreitol prior to SDS−PAGE resulted in the partial reduction of the cross-linker and a shift toward the lower-molecular mass forms, with the reappearance of some monomers.

Immunoprecipitation of the AQP4 Polypeptides from Rat Brain. Since AQP4 solubilized from rat cerebellum under nondenaturing conditions remains tetrameric, analysis of subunit composition is feasible. Peak sucrose gradient fractions were combined; immunoprecipitations were performed with either the N-terminal antibody or the C-terminal antibody, and immunoblots were probed with the C-terminal antibody. As expected, the C-terminal antibody recognizes both the 32 and 34 kDa polypeptides, and immunoprecipitates contain these polypeptides in ratios similar to those observed in whole tissues (Figure 6). The N-terminal antibody recognizes only the 34 kDa isoform, but immunoprecipitates contain both the 32 and 34 kDa polypeptides. Relative to the 32 kDa polypeptide, the abundance of the 34 kDa polypeptide was enriched in the N-terminal immunoprecipitates (ratio of 32 to 34 kDa of 1 to 0.33), indicating that whole cerebellum contains a population of 32 kDa homotetramers in addition to a population of heterotetramers containing 32 and 34 kDa subunits. Nonspecific IgG failed to precipitate AQP4.

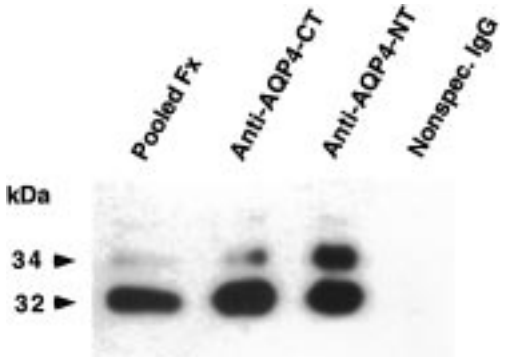

FIGURE 6: Coimmunoprecipitation of the AQP4 32 and 34 kDa polypeptides from rat brain. Sucrose gradient fractions were pooled and analyzed by SDS−PAGE. Immunoblotting was performed before or after immunoprecipitation with the C-terminal antibody (anti-AQP4-CT), the N-terminal antibody (anti-AQP4-NT), or rabbit nonspecific IgG. The immunoblot was probed with the C-terminal antibody.

Heterologous Expression of the 32 and 34 kDa Polypeptides. To evaluate determinants of AQP4 heterotetramer formation, *X. laevis* oocytes were injected with cRNAs for the M23 and M1 isoforms in varying ratios (3:1, 1:1, and 1:3). Three days after injection, membranes from these oocytes were solubilized in deoxycholate and quantitatively immunoprecipitated with either the N-terminal antibody or the C-terminal antibody to determine if the subunits reside within heterotetramers. Oocytes injected with M23 and M1 cRNAs in a 3:1 ratio expressed more 32 than 34 kDa polypeptide. Similar proportions were obtained when solubilized oocyte membranes were immunoprecipitated with either the N-terminal antibody or the C-terminal antibody and analyzed by immunoblotting (Figure 7A). The similar results with both antibodies indicate that the two different polypeptides reside within the same oligomers. Oocytes injected with equal amounts of M23 and M1 cRNAs yielded

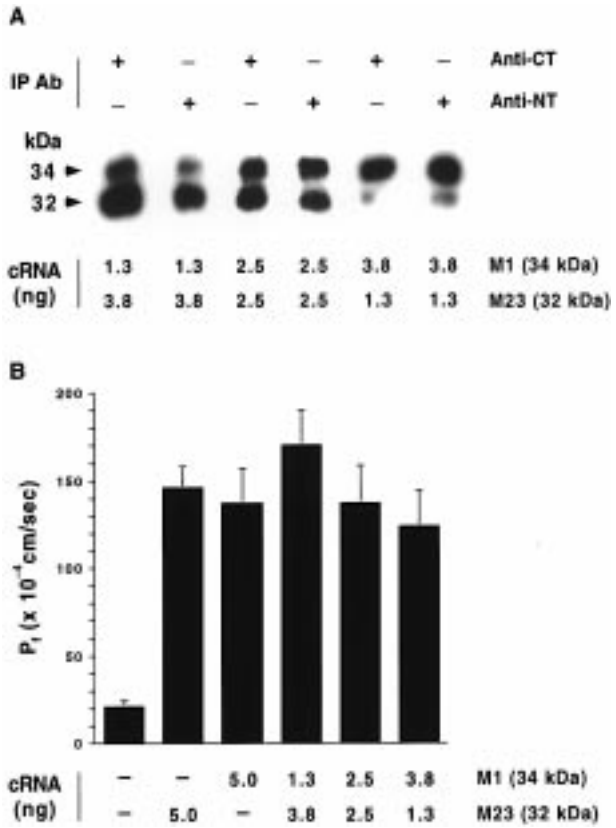

FIGURE 7: Heterotetramer formation and water permeability of AQP4 32 and 34 kDa polypeptides expressed in *X. laevis* oocytes. (A) Immunoprecipitation of AQP4 heterotetramers from oocytes expressing the 32 and 34 kDa polypeptides. Solubilized membranes from *Xenopus* oocytes injected with cRNA for the M23 and M1 transcripts were used for immunoprecipitation with the indicated C-terminal (anti-AQP4-CT) or N-terminal antibody (anti-AQP4−NT). Immunoprecipitates were analyzed by SDS−PAGE and immunoblotting with the C-terminal antibody. (B) Osmotic water permeability of oocytes expressing AQP4 32 and 34 kDa polypeptides. *Xenopus* oocytes were injected with the indicated amounts of AQP4 M23 and M1 cRNAs. The osmotic water permeability was measured 3 days later. Results from each series of oocytes were expressed as the mean P_f ($\times 10^{-4}$ cm/s) ± the standard deviation.

equivalent amounts of the 32 and 34 kDa polypeptides, and oocytes injected with M23 and M1 cRNAs in a 1:3 ratio expressed less 32 than 34 kDa polypeptide. Immunoprecipitations from both sets of oocytes also demonstrated that the 32 and 34 kDa polypeptides reside within the same oligomers. Thus, formation of AQP4 heterotetramers reflects the relative abundance of M1 and M23 polypeptides in the oocyte system.

Osmotic Water Permeabilities of AQP4 Homo- and Heterotetramers. Recognizing that *AQP4* expresses two overlapping polypeptides that co-oligomerize in vivo raises the question of whether the two isoforms are functionally distinct and whether they interact synergistically in regulating water permeability. The osmotic water permeability was examined in *Xenopus* oocytes injected with different ratios of M23 and M1 cRNA (Figure 7B) prior to the verification of polypeptide expression by immunoprecipitation and immunoblotting (Figure 7A). AQP4 homotetramers composed of either 32 or 34 kDa polypeptides exhibited comparable osmotic water permeabilities (Figure 7B), consistent with the findings of Jung et al. (*14*). Oocytes injected with AQP4 cRNAs encoding different combinations of M1 and M23 also exhibited comparable osmotic water permeabilities, with no synergistic effect noted. Thus, the biological need for the coexpression of 32 and 34 kDa polypeptides is not simply explained by differences in water permeation.

DISCUSSION

These studies demonstrate expression of four distinct AQP4 polypeptides in rat brain. The 32, 34, 36, and 38 kDa polypeptides were apparently not previously distinguished due to difficulties in AQP4 protein solubilization, limitations in electrophoretic resolution, and the lack of an N-terminal antibody. As reported here, preparation of SDS−PAGE samples at 37 °C prevented AQP4 aggregation, and including high concentrations of urea in the gels yielded significantly improved band resolution. The 32 kDa polypeptide corresponds to the M23 isoform, and the 34 kDa polypeptide corresponds to the M1 isoform (*14*). The 32 and 34 kDa polypeptides were observed in all the tissues that were analyzed, with the predominant polypeptide being the 32 kDa one. Although the 34 kDa polypeptide was especially visible in cerebellum and spinal cord, this may simply reflect the higher level of total AQP4 expression in these tissues, since immunoblot signals are not linearly related to protein concentrations.

The 38 kDa polypeptide is exceedingly scarce and, on the basis of immunoreactivity with the N-terminal antibody, is related to the 34 kDa polypeptide (M1 isoform), whereas the 36 kDa polypeptide is somewhat more abundant and related to the 32 kDa polypeptide (M23 isoform). *AQP4* encodes an N-linked glycosylation consensus site (N153, Figure 1), but interpretation of PNGase F digestion of cerebellum membranes was not possible. *AQP4* also encodes two protein kinase C (PKC) phosphorylation consensus sites (T107 and S180, Figure 1), and in vitro phosphorylation of AQP4 by PKC has recently been reported (*30*). Nevertheless, phosphatase treatment of cerebellum membranes prior to electrophoresis did not cause any disappearance of the 36 and 38 kDa bands, and treatment of AQP4-expressing oocytes with the PKC agonist phorbol 12,13-dibutyrate did not lead to their appearance. Although the presumed post-translational modification present on the 36 and 38 kDa polypeptides has not been firmly established, these comprise only a very small proportion of the total AQP4 protein mass.

AQP4 is known to be heavily expressed in astrocytes, where the C-terminal antibody produces immunogold labeling over perivascular endfeet in regions contacting the basement membrane (*21*, *22*). The N-terminal antibody also yields immunogold labeling in the same distribution but with a lower intensity (Figure 4). Thus, while the 32 and 34 kDa polypeptides are clearly differentially expressed, they do not appear to be differentially sorted. Extensive orthogonal arrays of intramembranous particles are found in perivascular astrocyte endfeet throughout the central nervous system as well as in astrocyte processes of the glia limitans beneath the pia. These arrays have been reported to increase in number in reactive astrocytes surrounding a brain injury (*31*) and disappear rapidly in response to hypoxia (*32*, *33*). Cells transfected with the M23 isoform of AQP4 were shown to contain orthogonal arrays (*34*), and direct labeling of orthogonal arrays in freeze-fracture replicas of astrocyte

endfeet was recently accomplished with the AQP4 C-terminal antibody (*35*), demonstrating that AQP4 is an astrocyte orthogonal array protein. Attempts to label orthogonal arrays in freeze-fracture replicas with the N-terminal antibody have so far not been successful (J. Rash and J. Neely, unpublished results). The inability to directly label orthogonal arrays with the N-terminal antibody may reflect the harshness of the technique, the lower affinity of the antibody, or the lower abundance of the 34 kDa polypeptide. Alternatively, it is possible that 34 kDa polypeptides are not present in orthogonal arrays. If correct, this distinction between AQP4 homotetramers containing only 32 kDa subunits and heterotetramers containing 32 and 34 kDa subunits could have biological significance.

We were not able to distinguish the 32 and 34 kDa polypeptides functionally. On the basis of measurements of osmotic water permeability in oocytes, there appear to be no significant differences in the water transport activities of AQP4 tetramers containing different compositions of the 32 and 34 kDa polypeptides. Nonetheless, the 32 and 34 kDa polypeptides may experience significantly different forms of regulation in their native tissues, and the gene promoters for the two isoforms were reported to have different transcriptional enhancers (*26*).

The extra 22 amino acids at the N-terminus of the 34 kDa polypeptide could be differentially regulated at the post-translational level. While the 32 and 34 kDa polypeptides exhibited no obvious differences in subcellular distribution in rat cerebellum under nonstressed conditions, the N-terminus could potentially contribute to a dynamic regulation of AQP4 during stress by influencing cellular sorting. The N-terminal FXXV (FKGV) and C-terminal YXXV (YMEV) and LI sequences present in AQP4 match critical internalization motifs present in the GLUT4 glucose transporter and other membrane proteins (*36*, *37*). C-Terminal (S/T)XV sequences have been implicated in the clustering and membrane organization of numerous channel proteins through binding to PDZ domain proteins (*38*). The C-terminal SSV in AQP4 may play a role in stabilizing AQP4 in macromolecular complexes with other proteins such as potassium channels (*39*). Thus, these sequences could be involved in regulating AQP4 targeting or degradation. Because the 32 and 34 kDa polypeptides form heterotetramers, even a relatively low level of 34 kDa polypeptide could be sufficient to confer binding to another cellular protein. The definition of potential binding partners and their roles in regulating AQP4 will require further investigation.

ACKNOWLEDGMENT

We thank Masato Yasui, Barbara L. Smith, and Mark A. Knepper for helpful discussions and valuable assistance. Core oocyte facilities were provided by Wm. B. Guggino (Department of Physiology, Johns Hopkins University School of Medicine).

REFERENCES

1. Agre, P., Bonhivers, M., and Borgnia, M. J. (1998) *J. Biol. Chem. 273*, 14659−14662.
2. Walz, T., Harai, T., Murata, K., Heymann, J. B., Mitsuoka, K., Fujiyoshi, Y., Smith, B. L., Agre, P., and Engel, A. (1997) *Nature 387*, 624−627.
3. Cheng, A., van Hoek, A. N., Yeager, M., Verkman, A. S., and Mitra, A. K. (1997) *Nature 387*, 627−630.
4. Li, H., Lee, S., and Jap, B. K. (1997) *Nat. Struct. Biol. 4*, 263−265.
5. Heymann, J. B., Agre, P., and Engel, A. (1998) *J. Struct. Biol. 121*, 191−206.
6. Froger, A., Tallur, B., Thomas, D., and Delamarche, C. (1998) *Protein Sci. 7*, 1458−1468.
7. Smith, B. L., and Agre, P. (1991) *J. Biol. Chem. 266*, 6407−6415.
8. Verbavatz, J. M., Brown, D., Sabolic, I., Valenti, G., Ausiello, D. A., van Hoek, A. N., Ma, T., and Verkman, A. S. (1993) *J. Cell Biol. 123*, 605−618.
9. Walz, T., Smith, B. L., Zeidel, M. L., Engel, A., and Agre, P. (1994) *J. Biol. Chem. 269*, 1583−1586.
10. Mathai, J. C., and Agre, P. (1999) *Biochemistry 38*, 923−928.
11. Jung, J. S., Preston, G. M., Smith, B. L., Guggino, W. B., and Agre, P. (1994*) J. Biol. Chem. 269*, 14648−14654.
12. Mulders, S. M., Bichet, D. G., Rijss, J. P., Kamsteeg, E. J., Arthus, M. F., Lonergan, M., Fujiwara, M., Morgan, K., Leijendekker, R., van der Sluijs, P., van Os, C. H., and Deen, P. M. (1998) *J. Clin. Invest. 102*, 57−66.
13. Hasegawa, H., Ma, T., Skach, W., Matthay, M. A., and Verkman, A. S. (1994*) J. Biol. Chem. 269*, 5497−5500.
14. Jung, J. S., Bhat, R. V., Preston, G. M., Guggino, W. B., Baraban, J. M., and Agre, P. (1994) *Proc. Natl. Acad. Sci. U.S.A. 91*, 13052−13056.
15. Frigeri, A., Gropper, M. A., Turck, C. W., and Verkman, A. S. (1995*) Proc. Natl. Acad. Sci. U.S.A. 92*, 4328−4331.
16. Frigeri, A., Gropper, M. A., Umenishi, F., Kawashima, M., Brown, D., and Verkman, A. S. (1995) *J. Cell Sci. 108*, 2993−3002.
17. Terris, J., Ecelbarger, C. A., Marples, D., Knepper, M. A., and Nielsen, S. (1995*) Am. J. Physiol. 269*, F775−F785.
18. Nielsen, S., King, L. S., Christensen, B. M., and Agre, P. (1997) *Am. J. Physiol. 273*, C1549−C1561.
19. Frigeri, A., Nicchia, G. P., Verbavatz, J. M., Valenti, G., and Svelto, M. (1998) *J. Clin. Invest. 102*, 695−703.
20. Koyama, Y., Yamamoto, T., Tani, T., Nihei, K., Kondo, D., Funaki, H., Yaoita, E., Kawasaki, K., Sato, N., Hatakeyama, K., and Kihara, I. (1999) *Am. J. Physiol. 276*, C621−C627.
21. Nielsen, S., Nagelhus, E. A., Amiry-Moghaddam, M., Bourque, C., Agre, P., and Ottersen, O. P. (1997) *J. Neurosci. 17*, 171−180.
22. Nagelhus, E. A., Veruki, M. L., Torp, R., Haug, F. M., Laake, J. H., Nielsen, S., Agre, P., and Ottersen, O. P. (1998) *J. Neurosci. 18*, 2506−2519.
23. Yang, B., Ma, T., and Verkman, A. S. (1995) *J. Biol. Chem. 270*, 22907−22913.
24. Lu, M., Lee, M. D., Smith, B. L., Jung, J. S., Agre, P., Verdijk, M. A. J., Merkx, G., Rijss, J. P. L., and Deen, P. M. T. (1996) *Proc. Natl. Acad. Sci. U.S.A. 93*, 10908−10912.
25. Turtzo, L. C., Lee, M. D., Lu, M., Smith, B. L., Copeland, N. G., Gilbert, D. J., Jenkins, N. A., and Agre, P. (1997) *Genomics 41*, 267−270.
26. Umenishi, F., and Verkman, A. S. (1998) *Genomics 50*, 373−377.
27. Laemmli, U. K. (1970) *Nature 227*, 680−685.
28. Preston, G. M., Carroll, T. P., Guggino, W. B., and Agre, P. (1992) *Science 256*, 385−387.
29. Preston, G. M., Jung, J. S., Guggino, W. B., and Agre, P. (1993) *J. Biol. Chem. 268*, 17−20.
30. Han, Z., Wax, M. B., and Patil, R. V. (1998) *J. Biol. Chem. 273*, 6001−6004.
31. Anders, J. J., and Brightman, M. W. (1982) *J. Neurocytol. 11*, 1009−1029.
32. Landis, D. M. D., and Reese, T. S. (1981) *J. Cell Biol. 88*, 660−663.
33. Cuevas, P., Diaz, J. A. G., Dujovny, M., Diaz, F. G., and Ausman, J. I. (1985) *Anat. Embryol. 172*, 171−175.

34. Yang, B., Brown, D., and Verkman, A. S. (1996) *J. Biol. Chem. 271*, 4577−4580.
35. Rash, J. E., Yasumura, T., Hudson, C. S., Agre, P., and Nielsen, S. (1998) *Proc. Natl. Acad. Sci. U.S.A. 95*, 11981−11986.
36. Sandoval, I. V., and Bakke, O. (1994) *Trends Cell Biol. 4*, 292−297.
37. Marks, M. S., Ohno, H., Kirchhausen, T., and Bonifacino, J. S. (1997) *Trends Cell Biol. 7*, 124−128.
38. Gee, S. H., Madhavan, R., Levinson, S. R., Caldwell, J. H., Sealock, R., and Froehner, S. C. (1998) *J. Neurosci. 18*, 128−137.
39. Nagelhus, E. A., Horio, Y., Inanobe, A., Fujita, A., Haug, F.-M., Nielsen, S., Kurachi, Y., and Ottersen, O. P. (1999) *Glia 26*, 47−54.

BI990941S